A suite of asymmetric citrate siderophores isolated from a marine *Shewanella* species

Jeffrey R. Carmichael, Hongjun Zhou, Alison Butler*

Department of Chemistry and Biochemistry, University of California, Santa Barbara, CA 93106-9510

*corresponding author: butler@chem.ucsb.edu, telephone: 805-893-8178, fax: 805-893-4120

Abstract

Woodybactins A-D are a suite of new fatty acyl siderophores produced by the luminous marine bacterium *Shewanella woodyi* MS32. While this bacterium has a set of genes homologous to the biosynthetic gene cluster for aerobactin, aerobactin is not produced. The arrangement of these genes within the genome differs in *S. woodyi* MS32 when compared to *E. coli* and other species producing siderophores similar to aerobactin, and one synthetase gene which would append a second acyl-hydroxylysine to the terminal carboxylate of citrate is not functional. Within the suite of woodybactins A-D, which differ by the fatty acid appendage, one contains an unusual C_9 (9:0) fatty acid and one contains a unique branched C_9 iso (9:0 iso) fatty acid, as well as a C_8 (8:0) and C_{10} (10:0) fatty acid.

Keywords

Shewanella woodyi MS32, siderophore, iron, biosynthesis, NIS synthetase

1. Introduction.

Bacteria generally require iron to grow. Many bacteria produce siderophores, low molecular weight Fe(III) chelators, to facilitate iron uptake. Siderophores are synthesized by well-defined pathways encoded in the bacterial genome. Peptidic siderophores are synthesized by **n**on**r**ibosomal **p**eptide **s**ynthetase (NRPS) enzymes.[1-3] Non-peptidic siderophores, such as aerobactin (Figure 1A), are synthesized by **N**RPS-**i**ndependent **s**iderophore (NIS) synthetases.[4] Aerobactin is produced by *E. coli*[5-6] as well as other pathogenic bacteria,[7] plant pathogens,[6] and marine *Vibrio* species.[8-9] In *E. coli*, aerobactin biosynthesis is encoded by the *iucABCD* gene cluster. IucD catalyzes the hydroxylation of the N_6 of L-lysine. IucB then catalyzes the N_6-acetylation of N_6-hydroxy-L-lysine. The synthetases IucA and IucC function sequentially to append N_6-acetyl-N_6-hydroxy-L-lysine to each terminal carboxylate of citrate, with IucA catalysis producing the S configuration at the central C-3 carbon of the citryl group (Figure 1B).[4-5, 10]

Ochrobactins A-C and ochrobactins-OH A-C are siderophores with structures resembling aerobactin, although both acetyl groups are replaced by fatty acids (Figure 2).[11-12] Fatty acid appendages, which are not uncommon in NIS siderophores, are also present in rhizobactin 1021[13] and the synechobactins.[14-15] Most of the acylated citrate-derived siderophores are asymmetric about the C-3 center of the citryl group as a result of two different fatty acid appendages, although ochrobactin C and ochrobactin-OH B are symmetric. Homologs of aerobactin's *iucB* biosynthesis gene append a fatty acyl chain and acetyl group to hydroxy-diaminopropane during synthesis of rhizobactin 1021,[16] although the specificity of *iucB* homologs for the fatty acid vs an acetyl group has not been elucidated.[13, 16] Branched fatty acids

have yet to be reported in siderophores, and odd-chain fatty acids have only been reported for the synechobactins and the peptidic mycobactin siderophores.[15, 17]

NIS synthetases are divided into three subfamilies of enzymes: Type A, B, and C NIS synthetases. Type A synthetases are specific for citric acid, Type B for α-ketoglutaric acid, and Type C for derivatives of citrate or succinate.[4, 18] Type A and C NIS synthetases are further divided into Types A, A', C, and C'. Little distinction exists between the function of Types A and A' NIS synthetases in that both typically catalyze amide bond formation between citric acid and an amine, although the Types A and A' are phylogenetically distinct (see below). Types C and C' also perform very similar functions through amide bond formation, although Type C' enzymes are also known to oligomerize and cyclize citryl or succinyl derivatives, forming siderophores such as desferrioxamines, alcaligin, avaroferrin, and putrebactin.[19-26]

Shewanella woodyi MS32 is a bioluminescent marine bacterium (Figure S1) originally isolated from the Alboran Sea, and named in honor of J. Woodland ("Woody") Hastings, a legend in the field of photobiology.[27] The bioluminescence of *S. woodyi* MS32 is under quorum sensing control.[27-29] *S. woodyi* species produce relatively high amounts of iso fatty acids as compared to *Vibrio* or *Photobacterium* species, and odd-chain fatty acids have also been reported in *S. woodyi* species.[27] The unusual fatty acid production of *S. woodyi* could indicate the production of novel fatty acid-containing metabolites.

The genome of *S. woodyi* MS32 contains genes homologous to the biosynthetic gene cluster for aerobactin, although the genes exist in a different spatial arrangement in the genome. Here we report the structures of woodybactins A-D, a suite of asymmetric citrate siderophores with structures similar to those of aerobactin, ochrobactins, and ochrobactins-OH, isolated from

Shewanella woodyi MS32. Woodybactin C contains the uncommon C_9 (9:0) fatty acid, and woodybactin B contains a unique iso-branched C_9 (9:0 iso) fatty acid.

2. Materials and Methods

2.1. General Experimental Procedures. All ^{1}H and two-dimensional (2D) NMR spectra were obtained at 25 °C using a Varian Inova 600 MHz NMR spectrometer equipped with an inverse detection probe. All ^{13}C NMR spectra were obtained at room-temperature (~23 °C) using a Varian Inova 500 MHz spectrometer equipped with a broadband probe. NMR samples were dissolved in dimethyl sulfoxide-d_6 (Cambridge Isotope Laboratories). All NMR spectra are referenced indirectly according to the signals from the solvent DMSO with the residual ^{1}H signal set to 2.54 ppm and ^{13}C signal set to 40.45 ppm. Molecular masses were determined using a Waters Xevo G2-XS QTof with positive mode electrospray ionization coupled to an ACQUITY UPLC-H-Class system with a Waters BEH C18 column. Samples were analyzed with a linear gradient of 0% to 100% CH_3CH (0.1% formic acid) in ddH_2O (0.1% formic acid) over 10 min.

2.2. Bacterial Growth and Isolation of Siderophores. *Shewanella woodyi* MS32 was grown in 2 liters of low-iron artificial seawater medium (ASG) containing 6 g Casamino acids, 30 g NaCl, 1.50 g KCl, 24 g $MgSO_4 \cdot 7H_2O$, 6 g $CaCl_2 \cdot 2H_2O$, 2 g NH_4Cl, 0.1 g Glycerol phosphate and 4 mL 1.0 M $NaHCO_3$ or Shewanella Marine Agar (SMA) containing (per liter) 5 g Bacto Peptone, 1 g Bacto Yeast Extract, 30.16 g NaCl, 5.08 g $MgCl_2 \cdot 6H_2O$, 6.16 g $MgSO_4 \cdot 7H_2O$, and 1.5 g KCl and brought to pH 7.5, with 15 g of bacto agar.[27] Media were inoculated with 5 mL of 2216 marine broth grown from a single colony of the bacterium isolated from a plate of SMA, shaken overnight at 180 rpm. The bacterial culture was grown on an orbital shaker at 180 rpm until it reached stationary phase as analyzed by the optical density at 600 nm versus growth time, at which point the cell culture gave a positive response to a chrome azurol-S (CAS) assay,

indicating the potential presence of siderophores.[30] The culture was centrifuged (6,000 rpm, 30 min, 4 °C) in an SLA-3000 rotor, the supernatant was decanted and mixed with ~200 mL (1/10 volume) of Amberlite XAD-2 resin (Supelco) and was shaken for ~4 hours at 120 rpm, until supernatant tested CAS-negative. The XAD-2 resin was then filtered and rinsed with 2 L doubly-deionized H_2O (Barnstead Nanopure II), and the siderophores were eluted with 100% MeOH. The CAS-positive MeOH fractions were consolidated and concentrated under vacuum to ~15 mL and were run through reverse-phase HPLC for purification using a gradient of 5% to 100% methanol over 50 minutes on a YMC 20 x 250 mm C18-AQ column. The cell pellets from centrifugation were resuspended in 70% ethanol (300 mL) and shaken at 4 °C for 24 hours, at which point they were centrifuged (6,000 rpm, 30 min, 4 °C) in an SLA-3000 rotor. The resulting supernatant was filtered through a 0.22 μm filter and concentrated under vacuum. The sample was then diluted in ~500 mL deionized H_2O and worked up with XAD-2 resin as described above.

3. Results and Discussion

3.1. Genome Mining

The genome of *S. woodyi* MS32 was screened for siderophore biosynthesis genes. While the genome lacks NRPS genes, it contains a set of genes homologous to *iucA*, *iucB*, *iucC*, and *iucD*, the cluster encoding biosynthesis of aerobactin, as well as *iutA*, the gene encoding the aerobactin transporter. However, the arrangement of the homologous genes in *S. woodyi* MS32, *swoA*, *swoB*, *swoC*, *swtA*, and *swoD,* differs from that in *E. coli* (Figure 3A, Table S1). In particular the *iucC* homolog, *swoD*, resides nearly 2.5 million base pairs downstream from the gene cluster of *swoABC* and *swtA* (Figure 3B).

Rhizobactin 1021 and the synechobactins are produced by NIS synthetases with homology to those of aerobactin[16, 31] (Figure 3A), although each citryl carboxylate group is derivatized with a different compound, producing asymmetric siderophores, unlike aerobactin. Rhizobactin 1021 and the synechobactins all have an acetyl appendage attached to hydroxy-diaminopropane on one side of the citryl group. On the opposing citryl carboxylate, rhizobactin 1021 has 2-decenoic acid appended to the hydroxy-diaminopropane,[13] and the synechobactins have fatty acids ranging from 8:0 to 16:0 appended to the hydroxy-diaminopropane.[14-15] The biosynthetic gene clusters for rhizobactin 1021 and synechobactins each contain two *iucB* homologs, presumably one for the acetyl group and one for the fatty acids.[4, 16, 31] The genome of *S. woodyi* MS32 contains only one *iucB* homolog, *swoB*.

3.2. Structure Determination

To isolate siderophores produced by *S. woodyi* MS32, the bacteria were grown as described in Materials and Methods. The HPLC trace of the *S. woodyi* MS32 supernatant extract contains four peaks (Figure 4), named here woodybactins A-D, which were identified as

potential siderophores using the chrome azurol-S (CAS) assay.[30] Electrospray UPLC-MS analysis showed compounds A-D having molecular ion peaks of m/z 463, 477, 477, and 491, respectively, while the mass for aerobactin, m/z 565, was not observed.[10] The mass difference of 14 between 463, 477, and 491 suggests a potential difference of a single CH_2 group. All four compounds have similar fragmentation patterns below m/z 337 (Figure S2), suggesting a major shared fragment between all of the woodybactins. The mass spectra of the woodybactins all share some fragments with the ochrobactins and ochrobactins-OH, including m/z 128, 145, and 163, which correspond to N_6-hydroxy-L-lysine.[11-12] Another indicative fragment for the woodybactins is N_6-hydroxy-L-lysine attached to an acyl group, indicated by the m/z 289 fragment in woodybactin A (also observed for ochrobactin B), m/z 303 in woodybactins B and C, and m/z 317 in woodybactin D (Figure 5, Figures S2-3).[11-12] For aerobactin-producing species, the related N_6-acetyl-N_6-hydroxy-L-lysine fragment is observed (m/z 205),[9] which was not observed in extracts of *S. woodyi* MS32. These data suggest woodybactins A-D contain fatty acid chains of mostly varying length, with two having the same mass (Figure 5, Figures S2-3).

NMR of woodybactins A-D established the presence of citrate and hydroxylysine, each with a different fatty acid appendage (Figure 6). All four siderophores have nearly identical resonances from C1 through C16 in both ^{13}C- and ^{1}H-NMR spectra (Table 1, Tables S2-S4). A triplet at 0.89 ppm integrates to 3 protons in the ^{1}H-NMR spectra of woodybactins A, C, and D and couples to only CH_2 carbons in the HMBC spectrum, indicating these siderophores all consist of straight-chain fatty acids. Woodybactin A has a C_8 8:0 fatty acid, woodybactin C has a C_9 9:0 fatty acid, and woodybactin D has a C_{10} 10:0 fatty acid. The ^{1}H-NMR spectrum of woodybactin B has a doublet at 0.88 ppm integrating to 6 protons (Table 1), corresponding to two CH_3 groups branched off of a CH, which was further confirmed through HMBC and COSY

(Figures S11-12). Furthermore, although the two branched CH_3 resonances overlap, each CH_3 group of protons couples with the other methyl ^{13}C via three-bond J coupling, giving an intense resonance in the HMBC spectrum at the CH_3 resonance position. This coupling pattern is indicative of an iso-fatty acid, and represents the first instance of a siderophore containing a branched fatty acid. Odd-chain fatty acids, as in woodybactin B have only been reported in a few other siderophores.[15, 17]

3.3. Phylogenetic analysis of *swoA* and *swoD*

The phylogeny of the synthetase genes *swoA* and *swoD* was compared to other NIS synthetases with known functions (Figure 7). The phylogenetic tree shows that *swoA* groups within the Type A clade alongside *iucA*, and *swoD* groups within the C' clade with *iucC* (Figure 7). Given the function of Type A NIS synthetases to condense an amine or alcohol with citric acid, SwoA is predicted to catalyze the formation of a monosubstituted citryl product. As a member of the Type C' clade, SwoD is predicted to catalyze the condensation of an amine substituent to a monosubstituted citryl or succinyl group to form a disubstituted product.[19]

The activity of SwoD in *S. woodyi* MS32 is not apparent given the lack of a disubstituted citryl product similar to aerobactin, ochrobactins, and ochrobactins-OH.[11-12] No siderophores containing a disubstituted citryl were found in either the cell pellet (extraction outlined in Materials and Methods) or supernatant, which suggests that *swoD* is not operative in the biosynthesis of the woodybactins. However, unlike the other Type A NIS synthetases, SwoA appears to be attaching substrates with a range of fatty acid lengths to citric acid, indicating a relatively loose substrate specificity with respect to the nature of the fatty acids. The synechobactins contain a range of fatty acid lengths as well, which indicates a wide substrate specificity of its *iucA* homolog and potentially its two *iucB* homologs, although the biosynthesis of the synechobactins has not been extensively investigated.[31] The ochrobactins and ochrobactins-OH also contain a variety of fatty acid lengths, although the genomes of the bacteria which make them have not been published.[11-12] With more bacterial genomes being sequenced and made available, further investigations into these NIS biosynthetic pathways can hopefully soon be performed.

3.4. Fe(III) binding

Most siderophores coordinate Fe(III) with three bidentate ligands, commonly catechols, α-hydroxycarboxylic acids, and hydroxamic acids, with 1:1 stoichiometry. Some siderophores with two bidentate ligands, such as the bis hydroxamate putrebactin, and alcigin, bind Fe(III) with 1:1 or 2:3 Fe(III)-siderophore stoichiometry depending on pH conditions.[25, 39-41] Unfortunately Fe(III) titration of woodybactin B was hampered by precipitation. However, under conditions of ~0.3 Fe(III):woodybactin B the UV-visible spectrum of Fe(III)-woodybactin B in 0.1 M phosphate buffer pH 7, shows an absorption maximum at ~420 nm with a shoulder at ~280 nm (Figure S21), indicating coordination by both the hydroxamate and α-hydroxycarboxylate. Similar absorption maxima are observed for aerobactin.[9] UV photolysis of Fe(III)-woodybactin B leads to loss of 46 mass units, consistent with the coordination of α-hydroxy carboxylate to Fe(III) (Figure S22).[9]

4. Conclusions

A suite of four fatty acyl siderophores, woodybactins A-D, have been isolated from *Shewanella woodyi* MS32. The woodybactins differ only in their fatty acid appendages, one of which, woodybactin C, has an uncommon odd-chain 9:0 fatty acid, one of which, woodybactin B, has a 9:0 iso branched fatty acid. Iso branched fatty acids have not been reported previously in siderophores.

The woodybactin structures were partially predicted through genome mining of *S. woodyi* MS32. The genome contains the biosynthesis genes *swoABC* and *swoD*, and the siderophore transporter *swtA*. The *swoABC* and *swoD* genes are homologous to the biosynthesis genes for

aerobactin, *iucABCD*. SwoA is a Type A siderophore synthetase closely related to IucA, whose function is to append N_6-acetyl-N_6-hydroxy-L-lysine to a citryl group, which gives us woodybactins A-D. SwoD is a Type C' siderophore synthetase closely related to IucC, and is predicted to append a second N_6-acetyl-N_6-hydroxy-L-lysine the monosubstituted citryl product of SwoA. The absence of a disubstituted citryl siderophore from *S. woodyi* MS32 indicates *swoD* is not functional with *swoABC*.

5. Acknowledgments

We thank Prof. Jeffrey Gralnick (University of Minnesota) for the sample of *Shewanella woodyi* MS32. A.B. gratefully acknowledges support from NSF CHE-1710761

6. References

1. Marahiel, M. A.; Stachelhaus, T.; Mootz, H. D., Modular Peptide Synthetases Involved in Nonribosomal Peptide Synthesis. *Chemical Reviews* **1997,** *97* (7), 2651-2674.

2. Stachelhaus, T.; Mootz, H. D.; Marahiel, M. A., The specificity-conferring code of adenylation domains in nonribosomal peptide synthetases. *Chemistry & Biology* **1999,** *6* (8), 493-505.

3. Grünewald, J.; Marahiel, M. A., Chemoenzymatic and Template-Directed Synthesis of Bioactive Macrocyclic Peptides. *Microbiology and Molecular Biology Reviews* **2006,** *70* (1), 121-146.

4. Challis, G. L., A Widely Distributed Bacterial Pathway for Siderophore Biosynthesis Independent of Nonribosomal Peptide Synthetases. *ChemBioChem* **2005,** *6* (4), 601-611.

5. de Lorenzo, V.; Bindereif, A.; Paw, B. H.; Neilands, J. B., Aerobactin biosynthesis and transport genes of plasmid ColV-K30 in Escherichia coli K-12. *Journal of Bacteriology* **1986,** *165* (2), 570-578.

6. Neilands, J. B., Mechanism and regulation of synthesis of aerobactin in Escherichia coli K12 (pColV-K30). *Canadian Journal of Microbiology* **1992,** *38* (7), 728-33.

7. Gibson, F.; Magrath, D. I., The isolation and characterization of a hydroxamic acid (aerobactin) formed by Aerobacter aerogenes 62-I. *Biochim. Biophys. Acta* **1969,** *192* (2), 175-184.

8. Haygood, M. G.; Holt, P. D.; Butler, A., Aerobactin production by a planktonic marine Vibrio sp. *Limnology and Oceanography* **1993,** *38* (5), 1091-1097.

9. Küpper, F. C.; Carrano, C. J.; Kuhn, J.-U.; Butler, A., Photoreactivity of Iron(III)−Aerobactin: Photoproduct Structure and Iron(III) Coordination. *Inorganic Chemistry* **2006,** *45* (15), 6028-6033.

10. Bailey, D. C.; Alexander, E.; Rice, M. R.; Drake, E. J.; Mydy, L. S.; Aldrich, C. C.; Gulick, A. M., Structural and functional delineation of aerobactin biosynthesis in hypervirulent Klebsiella pneumoniae. *Journal of Biological Chemistry* **2018,** *293* (20), 7841-7852.

11. Martin, J. D.; Ito, Y.; Homann, V. V.; Haygood, M. G.; Butler, A., Structure and membrane affinity of new amphiphilic siderophores produced by Ochrobactrum sp. SP18. *JBIC Journal of Biological Inorganic Chemistry* **2006,** *11* (5), 633-641.

12. Gauglitz, J. M.; Zhou, H.; Butler, A., A suite of citrate-derived siderophores from a marine Vibrio species isolated following the Deepwater Horizon oil spill. *Journal of Inorganic Biochemistry* **2012,** *107* (1), 90-95.

13. Persmark, M.; Pittman, P.; Buyer, J. S.; Schwyn, B.; Gill, P. R.; Neilands, J. B., Isolation and structure of rhizobactin 1021, a siderophore from the alfalfa symbiont Rhizobium meliloti 1021. *Journal of the American Chemical Society* **1993,** *115* (10), 3950-3956.

14. Ito, Y.; Butler, A., Structure of synechobactins, new siderophores of the marine cyanobacterium Synechococcus sp. PCC 7002. *Limnology and Oceanography* **2005,** *50* (6), 1918-1923.

15. Boiteau, R. M.; Repeta, D. J., An extended siderophore suite from Synechococcus sp. PCC 7002 revealed by LC-ICPMS-ESIMS. *Metallomics* **2015,** *7* (5), 877-884.

16. Lynch, D.; O'Brien, J.; Welch, T.; Clarke, P.; Cuív, P. O.; Crosa, J. H.; O'Connell, M., Genetic organization of the region encoding regulation, biosynthesis, and transport of rhizobactin 1021, a siderophore produced by Sinorhizobium meliloti. *Journal of Bacteriology* **2001,** *183* (8), 2576-2585.

17. Snow, G. A., Mycobactins: iron-chelating growth factors from mycobacteria. *Bacteriological Reviews* **1970,** *34* (2), 99-125.

18. Oves-Costales, D.; Kadi, N.; Challis, G. L., The long-overlooked enzymology of a nonribosomal peptide synthetase-independent pathway for virulence-conferring siderophore biosynthesis. *Chemical Communications* **2009,** (43), 6530-6541.

19. Moore, M. M., Ironing out siderophore biosynthesis: a review of non-ribosomal peptide synthetase (NRPS)-independent siderophore synthetases AU - Carroll, Cassandra S. *Critical Reviews in Biochemistry and Molecular Biology* **2018,** *53* (4), 356-381.

20. Karimi, K. L.; Hoffmann, K. M., Determining the Structure of NRPS-Independent Siderophore (NIS) Synthetase DesD Using X-ray Crystallography. *The FASEB Journal* **2016,** *30* (1_supplement), 836.4-836.4.

21. Rütschlin, S.; Böttcher, T., Dissecting the Mechanism of Oligomerization and Macrocyclization Reactions of NRPS-Independent Siderophore Synthetases. *Chemistry – A European Journal* **2018,** *24* (60), 16044-16051.

22. Nishio, T.; Tanaka, N.; Hiratake, J.; Katsube, Y.; Ishida, Y.; Oda, J., Isolation and structure of the novel dihydroxamate siderophore alcaligin. *Journal of the American Chemical Society* **1988,** *110* (26), 8733-8734.

23. Giardina, P. C.; Foster, L.-A.; Toth, S. I.; Roe, B. A.; Dyer, D. W., Analysis of the alcABC operon encoding alcaligin biosynthesis enzymes in Bordetella bronchiseptica. *Gene* **1997,** *194* (1), 19-24.

24. Kadi, N.; Arbache, S.; Song, L.; Oves-Costales, D.; Challis, G. L., Identification of a Gene Cluster That Directs Putrebactin Biosynthesis in Shewanella Species: PubC Catalyzes Cyclodimerization of N-Hydroxy-N-succinylputrescine. *Journal of the American Chemical Society* **2008,** *130* (32), 10458-10459.

25. Codd, R.; Soe, C. Z.; Pakchung, A. A. H.; Sresutharsan, A.; Brown, C. J. M.; Tieu, W., The chemical biology and coordination chemistry of putrebactin, avaroferrin, bisucaberin, and alcaligin. *JBIC Journal of Biological Inorganic Chemistry* **2018,** *23* (7), 969-982.

26. Codd, R.; Richardson-Sanchez, T.; Telfer, T. J.; Gotsbacher, M. P., Advances in the Chemical Biology of Desferrioxamine B. *ACS Chemical Biology* **2018,** *13* (1), 11-25.

27. Makemson, J. C.; Fulayfil, N. R.; Landry, W.; Van Ert, L. M.; Wimpee, C. F.; Widder, E. A.; Case, J. F., Shewanella woodyi sp. nov., an Exclusively Respiratory Luminous Bacterium Isolated from the Alboran Sea. *International Journal of Systematic and Evolutionary Microbiology* **1997,** *47* (4), 1034-1039.

28. Liu, N.; Xu, Y.; Hossain, S.; Huang, N.; Coursolle, D.; Gralnick, J. A.; Boon, E. M., Nitric Oxide Regulation of Cyclic di-GMP Synthesis and Hydrolysis in Shewanella woodyi. *Biochemistry* **2012,** *51* (10), 2087-2099.

29. Tian, X.; Zhao, F.; You, L.; Wu, X.; Zheng, Z.; Wu, R.; Jiang, Y.; Sun, S., Interaction between in vivo bioluminescence and extracellular electron transfer in Shewanella woodyi via charge and discharge. *Physical Chemistry Chemical Physics* **2017,** *19* (3), 1746-1750.

30. Schwyn, B.; Neilands, J. B., Universal chemical assay for the detection and determination of siderophores. *Analytical Biochemistry* **1987,** *160* (1), 47-56.

31. Ludwig, M.; Bryant, D. A., Acclimation of the Global Transcriptome of the Cyanobacterium Synechococcus sp. Strain PCC 7002 to Nutrient Limitations and Different Nitrogen Sources. *Frontiers in Microbiology* **2012,** *3*, 145-145.

32. Berti, A. D.; Thomas, M. G., Analysis of achromobactin biosynthesis by Pseudomonas syringae pv. syringae B728a. *Journal of Bacteriology* **2009,** *191* (14), 4594-4604.

33. Lee, J. Y.; Janes, B. K.; Passalacqua, K. D.; Pfleger, B. F.; Bergman, N. H.; Liu, H.; Håkansson, K.; Somu, R. V.; Aldrich, C. C.; Cendrowski, S.; Hanna, P. C.; Sherman, D. H., Biosynthetic Analysis of the Petrobactin Siderophore Pathway from Bacillus anthracis. *Journal of Bacteriology* **2007,** *189* (5), 1698.

34. Barona-Gómez, F.; Wong, U.; Giannakopulos, A. E.; Derrick, P. J.; Challis, G. L., Identification of a Cluster of Genes that Directs Desferrioxamine Biosynthesis in Streptomyces coelicolor M145. *Journal of the American Chemical Society* **2004,** *126* (50), 16282-16283.

35. Sullivan, J. T.; Jeffery, E. F.; Shannon, J. D.; Ramakrishnan, G., Characterization of the siderophore of Francisella tularensis and role of fslA in siderophore production. *Journal of Bacteriology* **2006,** *188* (11), 3785-3795.

36. Allard, K. A.; Viswanathan, V. K.; Cianciotto, N. P., lbtA and lbtB Are Required for Production of the Legionella pneumophila Siderophore Legiobactin. *Journal of Bacteriology* **2006,** *188* (4), 1351-1363.

37. Tanabe, T.; Funahashi, T.; Nakao, H.; Miyoshi, S.-I.; Shinoda, S.; Yamamoto, S., Identification and characterization of genes required for biosynthesis and transport of the siderophore vibrioferrin in Vibrio parahaemolyticus. *Journal of Bacteriology* **2003,** *185* (23), 6938-6949.

38. Cheung, J.; Beasley, F. C.; Liu, S.; Lajoie, G. A.; Heinrichs, D. E., Molecular characterization of staphyloferrin B biosynthesis in Staphylococcus aureus. *Molecular Microbiology* **2009,** *74* (3), 594-608.

39. Ledyard, K. M.; Butler, A., Structure of putrebactin, a new dihydroxamate siderophore produced by Shewanella putrefaciens. *JBIC Journal of Biological Inorganic Chemistry* **1997,** *2* (1), 93-97.

40. Hou, Z.; Sunderland, C. J.; Nishio, T.; Raymond, K. N., Preorganization of Ferric Alcaligin, Fe2L3. The First Structure of a Ferric Dihydroxamate Siderophore. *Journal of the American Chemical Society* **1996,** *118* (21), 5148-5149.

41. Hou, Z.; Raymond, K. N.; O'Sulliva, B.; Esker, T. W.; Nishio, T., A Preorganized Siderophore: Thermodynamic and Structural Characterization of Alcaligin and Bisucaberin, Microbial Macrocyclic Dihydroxamate Chelating Agents1. *Inorganic Chemistry* **1998,** *37* (26), 6630-6637.

Table 1. NMR data of woodybactin B.

	δ_C, type	**δ_H (J in Hz)**	**COSY**	**HMBC**
1	172.2, C			
2	44.0, CH_2	2.68 m		1, 3, 4, 5
3	73.6, C			
4	175.7, C			
5	44.0, CH_2	2.68 m		2, 3, 4, 6
6	170.2, C			
N1		8.14 (d, 1H, J = 7.8)	7	6, 7
7	52.5, CH	4.17 (td, 1H, J = 5.1, 8.3)	N1, 9	8, 9
8	174.3, C			
9	31.7, CH_2	1.60 (m, 1H), 1.71 (m, 1H)	7, 10	7, 8, 10, 11
10	23.3, CH_2	1.30 m	9, 11	7, 9, 11, 12
11	26.9, CH_2	1.53 m	10, 12	9, 10, 12
12	47.8, CH_2	3.49 (t, 2H, J = 7.1 Hz)	11	10, 11, 13
N2				
13	173.6, C			
14	32.6, CH_2	2.36 (t, 2H, J = 7.6 Hz)	15	13, 15, 16
15	25.2, CH_2	1.51 m	14, 16	13, 14, 16, 17
16	30.0, CH_2	1.28 m	15	17, 18
17	27.6, CH_2	1.28 m	18	16, 18, 19
18	39.3, CH_2	1.17 (q, 2H, J = 6.9 Hz)	17, 20/20’	16, 17, 19, 20, 20’
19	28.3, CH	1.54 m		17, 18, 20, 20’
20, 20’	23.5, $2CH_3$	0.88 (d, 6H, J = 6.6 Hz)		18, 19, 20, 20’

Figure 1. A) Structure of aerobactin. B) Biosynthesis of aerobactin by IucABCD.[4-5, 10]

Figure 2. Structure of A) ochrobactins A, B. and C,[11] and B) ochrobactins-OH A, B, and C.[12]

Figure 3. A) Biosynthetic gene clusters of aerobactin and rhizobactin 1021, and predicted gene clusters of synechobactins (located on pAQ7 plasmid of *Synechococcus sp.* PCC7002) and woodybactins. The homologous genes to aerobactin in gene clusters of rhizobactin 1021 and woodybactin are placed in parentheses below the relevant gene. B) Relative locations of *swoABC, swtA*, and *swoD* in the *S. woodyi* MS32 genome.

Figure 4. HPLC chromatogram from supernatant of *S. woodyi* MS32. Sample is monitored at 215 nm.

Figure 5. Mass fragments of woodybactin A indicating a citrate appended by one acyl-hydroxylysine.

Figure 6. Structures of woodybactins A-D.

Figure 7. Phylogenetic analysis of several common NIS synthetases. AcsA and AcsD - achromobactin biosynthesis;[32] AsbA and AsbB - petrobactin biosynthesis;[33] DesD - desferrioxamine biosynthesis;[34] FslA - rhizoferrin biosynthesis;[35] IucA and IucC - aerobactin biosynthesis;[5] SwoA and SwoD - woodybactin biosynthesis (this work); LbtA - legiobactin biosynthesis;[36] PubC - putrebactin biosynthesis;[24] PvsB and PvsD - vibrioferrin biosynthesis;[37] RhbC - rhizobactin 1021 biosynthesis;[16] SbnE and SbnF - staphyloferrin B biosynthesis.[38]

Figure 1

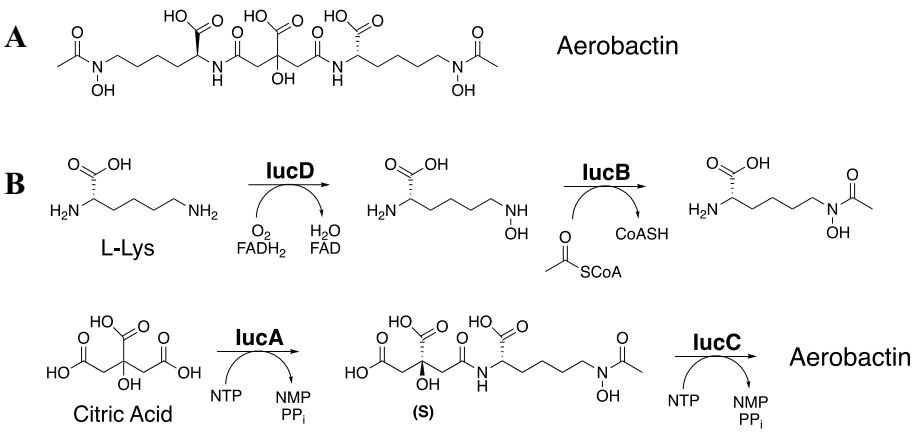

Figure 2

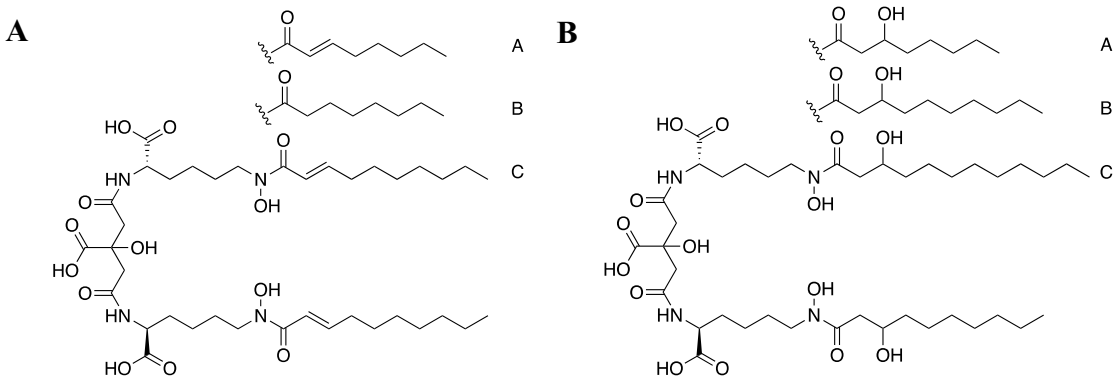

Figure 3

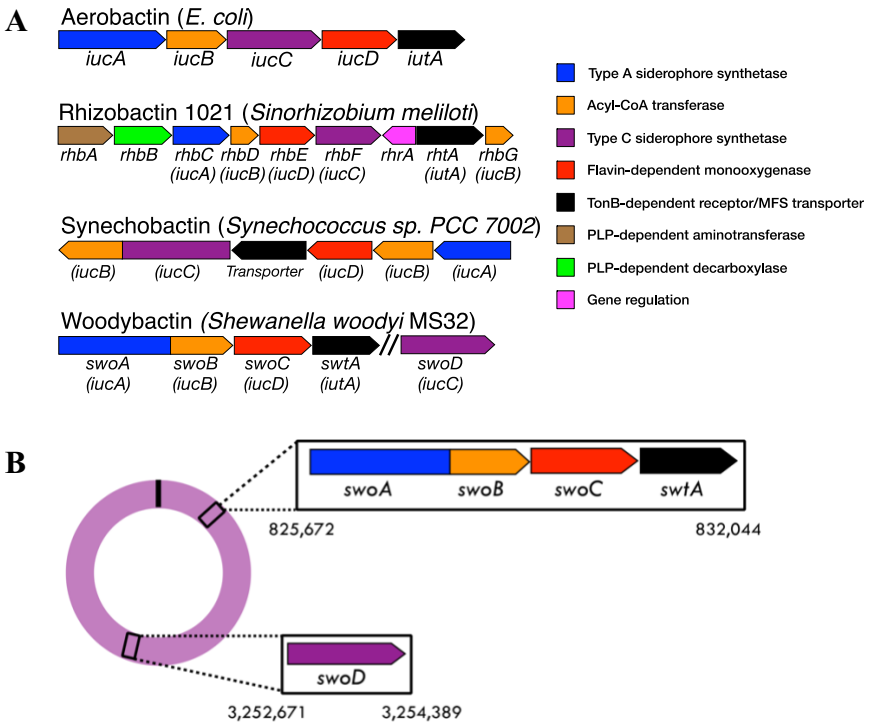

Figure 4

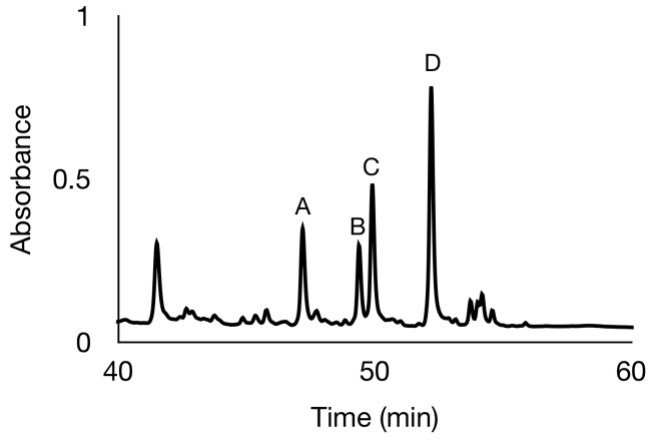

Figure 5

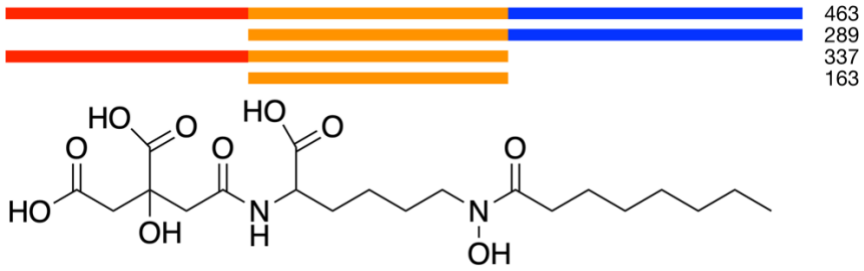

Figure 6

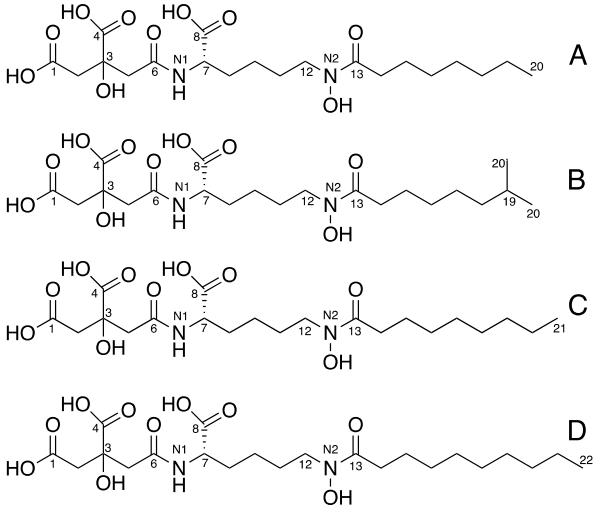

Figure 7

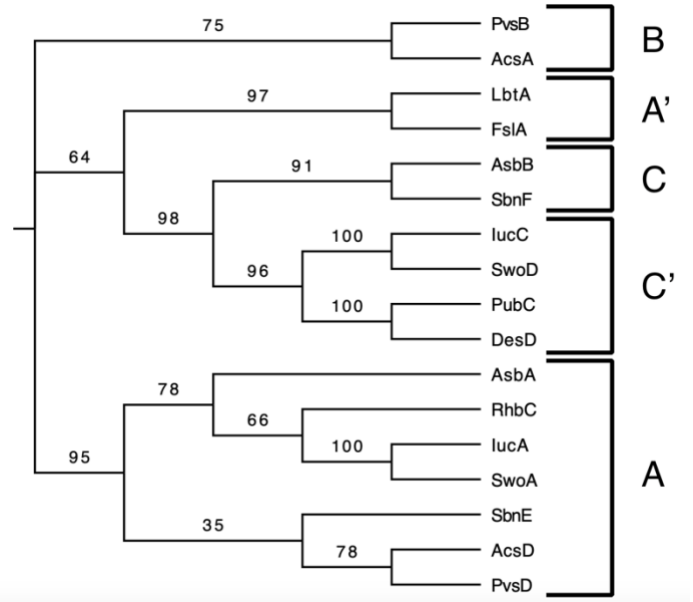
75
97
64
91
98
100
96
100
78
66
100
95
35
78
PvsB
AcsA
LbtA
FslA
AsbB
SbnF
IucC
SwoD
PubC
DesD
AsbA
RhbC
IucA
SwoA
SbnE
AcsD
PvsD
B
A'
C
C'
A